Elasto-Plastic Cyclic Horizontal Sway Behaviour of Wide Flange Unit Rigid Frames Subjected to Constant Vertical Loads

Comportement élasto-plastique de cadres rigides formés de profils à ailes larges soumis à des charges verticales constantes

Elasto-plastisches zyklisch horizontales Schwingungsverhalten von Rahmen aus Breitflanschprofilen unter konstanter vertikaler Last

Minoru YAMADA Professor Dr.-Ing.
Bunzo TSUJI Ass. Prof. Dipl.-Ing.
Yasuyuki MURAZUMI Dipl.-Ing.
Department of Architecture, Faculty of Engineering
Kobe University
Kobe, Japan

1. INTRODUCTION

In order to make clear the elasto-plastic cyclic deformation behavior of steel structures, various constant deflection amplitude tests are carried out on the unit rectangular steel rigid frames as a basic element of the steel structures. Analysis are developed with the special consideration on the Bauschinger effect and compared with test results.

2. ANALYSIS

2.1. The Bauschinger Model

The Bauschinger effect plays an important role on the deformation characteristics of the steel structures under the cyclic loads. Its effect is considered here using the Bauschinger model such as shown in Fig.2. The material (steel) is assumed to be composed of three different mechanical properties such as shown in Fig.2. With this model, the cyclic stress-strain relationship obtained is tri-linear type such as shown in Fig.3. The Bauschinger effect appears when the plastic deformation occurs at the opposite direction as the original one. Therefore the bi-linear type of the stress-strain relationship as shown in Fig.1 is applied initially.

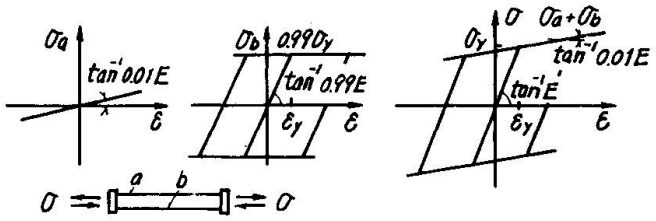

Fig.1 Bi-linear model [1)]

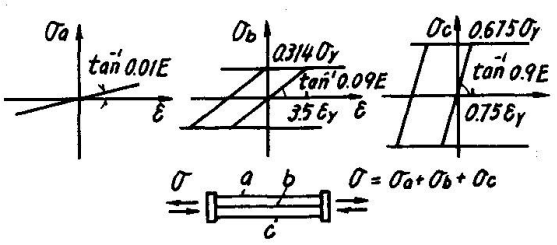

Fig.2 Bauschinger model

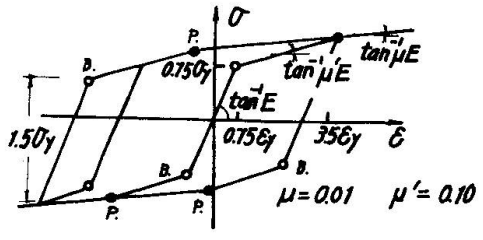

Fig.3 σ-ε relation

2.2. Deformation Analysis

The following assumptions are applied for the analysis:

(1) Wide flange section is simplified into the equivalent three points model[1] with the same cross sectional area, moment of inertia and fully plastic moment as the original one such as shown in Fig.4,

(2) Cyclic stress-strain relationships are defined intially by the bi-linear[1] model and subsequently by the Bauschinger model*,

(3) Plane section remains plane during deformation,

(4) The effect of shearing stress is not considered.

The non-dimensional stress-strain relations of each point are shown in the following equations according to the states of stress,

$q_i = e_i - e_{pi}$; elastic (1a),

$q_i = 1 + \mu(e_i - 1)$; tens. plastic (1b),

$q_i = -1 + \mu(e_i - 1)$; comp. plastic (1c),

$q_i = 1 - 0\mu(e_i - e_{pi}) + \alpha_i(1 - 10\mu)$; tens. Bauschinger (1d),

$q_i = 10\mu(e_i - e_{pi}) - (1.5 - \alpha_i)(1 - 10\mu)$; comp. Bauschinger (1e),

where $q_i = \sigma_i/\sigma_y$ and $e_i = \varepsilon_i/\varepsilon_y$, (i=1,2,3).

The equations of the equilibrium for the axial force N=nNy and the bending moment M=mMy are as follows,

$n = (q_1 + kq_2 + q_3)/(2+k)$ (2a),

$m = (q_1 - q_3)/2$ (2b).

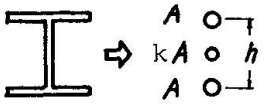

Fig.4 Three points model[1]

The stresses are composed of the elastic stress q_{ie}, that is proportional to the generalized stresses, m and n, and the residual stress q_{ir} as shown in Fig.5.

$q_{1e} = n + m$ (3a),

$q_{2e} = n$ (3b),

$q_{3e} = n - m$ (3c),

$q_{1r} = q_{3r} = \xi$ (4a),

$q_{2r} = -2\xi/k$ (4b).

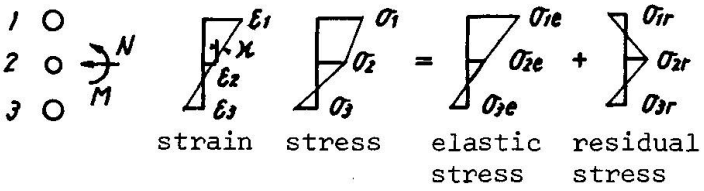

Fig.5 Strain and stress distributions

Indicating the subsequent yield stress $\bar{\sigma}_y = \alpha\,\sigma_y$ after the plastic deformation occured, the yield conditions of each point are for the bi-linear model

$\alpha_i - 2 \le q_i \le \alpha_i$ (i=1,2,3) (5),

and for the Bauschinger model

$\alpha_i - 1.5 \le q_i \le \alpha_i$ (i=1,2,3) (6).

Fig.6 shows the convex yield polygons composed of the three pairs of the parallel lines, where ξ is the parameter indicating the magnitude of the residual stress. The strain distribution of the cross section is determined by the strain of the centroidal axis $\varepsilon_2 = e_2\,\varepsilon_y$ and the curvature $\varkappa = e_\varkappa 2\,\varepsilon_y/h$ as follows:

(7a),

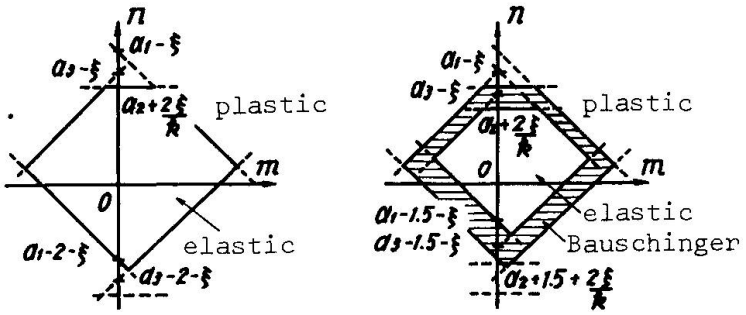

Fig.6 Yield conditions

* Recently after the completion of this analysis, a similar model was presented.[2]

$e_\beta = e_\gamma - e_\kappa$ (7c).

The stress-strain relationships of each point are obtained from the yield conditions which are determined considering the strain history of the cross section. With these relations and eq.(7), the strain distribution e_γ and e_κ of the cross section corresponding to the generalized stress m and n, are able to be obtained. Deformation analysis is carried out by the numerical integration procedures, dividing the columns and beams of the model frame, as shown in Fig.7, into thirty line elements which deform parabolically and satisfying the equilibrium conditions at each nodal point. The computed load deflection relations are shown in Fig.10 by broken lines. The black and white circles, • and ○, indicate the intiation of yielding and Bauschinger effect at the column end respectively. The dotted lines show the bi-linear model analysis [1] for comparison.

3. TESTS

3.1. Test Specimens and Test Series

Test specimens are made of rolled wide flange profils with welded joints and with stiffeners in each joint (see Fig.7). Tests are carried out on the various constant relative story displacement amplitudes of ±1.0cm, ±2.0cm and ±4.0cm under the action of the various constant vertical loads of the column of 0Ny, 1/3Ny and 1/2Ny, where Ny is the yield axial load of the column.

3.2. Loading and Measuring System

The specimen is set in the loading frame through pin roller supports, consisting of the needle roller bearings in each corner such as shown in Fig.8. In order to avoid lateral buckling, the beams are supported by the roller bearings. The vertical load is applied by the testing machine through the flat cage needle roller bearings, with a friction coefficient of 1/1000, inserted between the cross head and the loading frame. The lateral force is applied diagonally by the oil jack with load cell through the steel rods. The deflections are measured by dial gages and the strain distributions by wire strain gages.

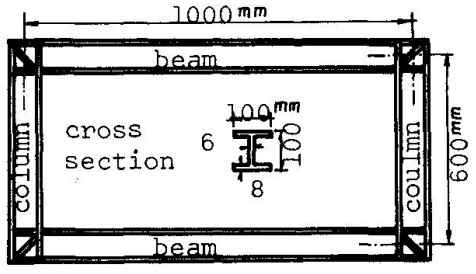

Fig.7 Specimen

Table 1 Test series

N/Ny	Displacement amplitude (cm)	Number of cycles
0	±2.0	4
1/3	±1.0	51
	±2.0	4
	±4.0	1
1/2	±1.0	10
	±2.0	4
	±4.0	1

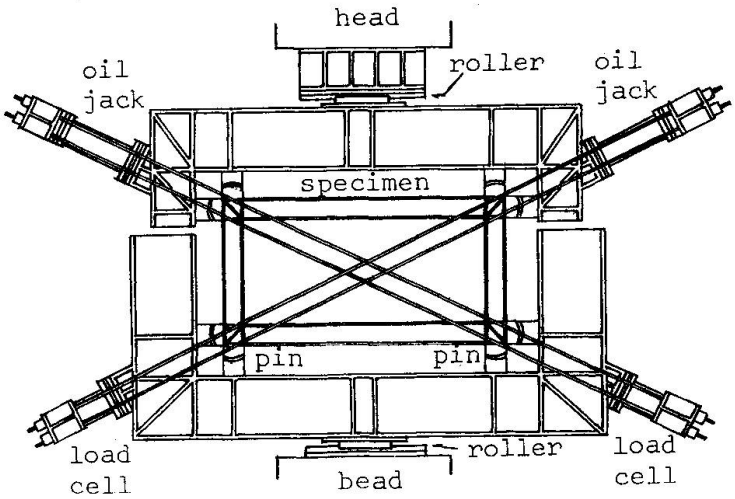

Fig.8 Loading system

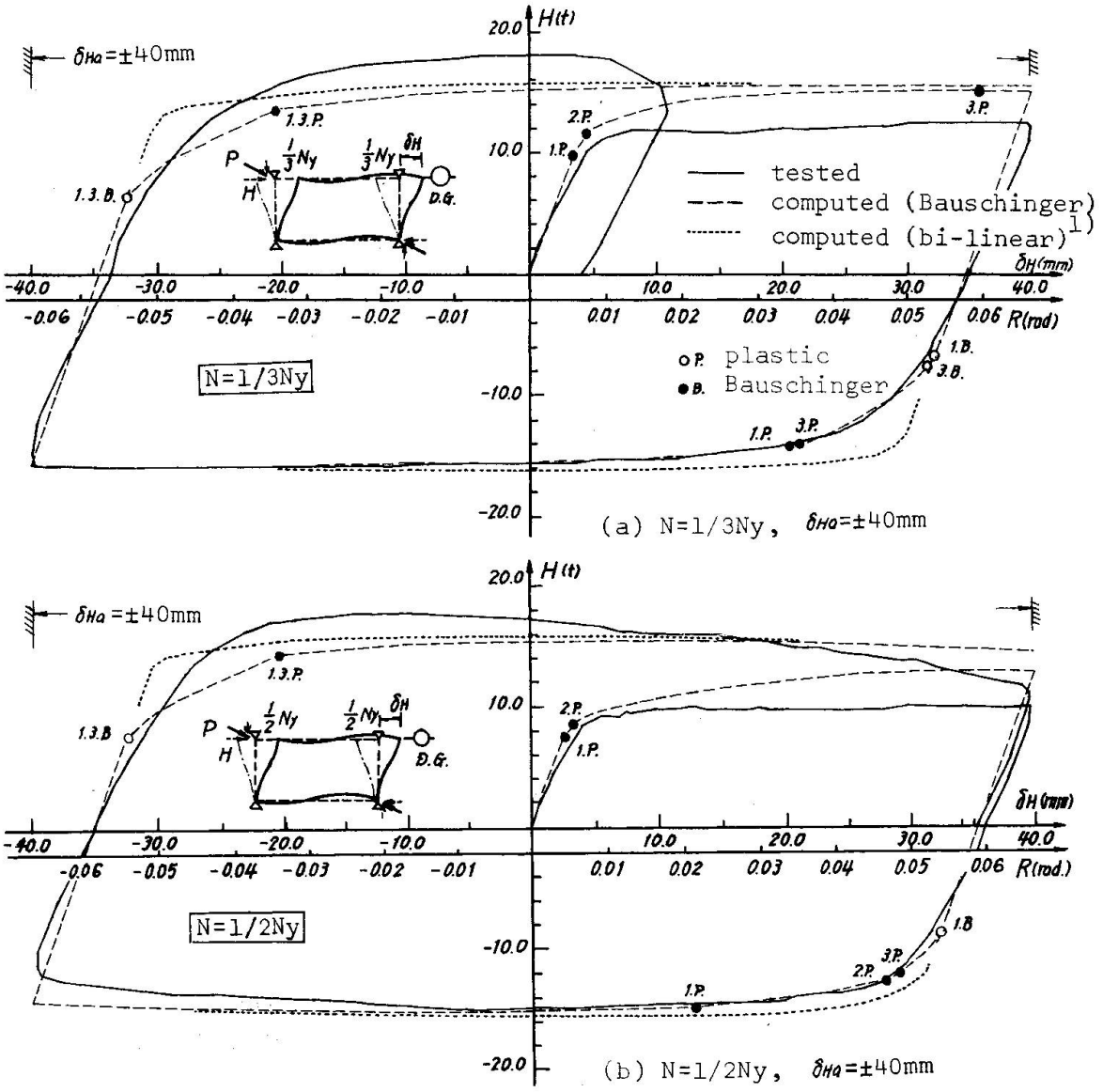

Fig.9 Load-Deflection Relationships

3.3. Test Results

The load deflection curves are shown in Fig.9 with solid lines. The relations between the sway amplitudes and the number of cycles until fracture is shown in Fig.10. The increases of the resistance with the increase of the number of cycles are shown in Fig.11.

4. DISCUSSIONS AND CONCLUDING REMARKS

4.1. Load Deflection Relationships

Fig.9 shows the load deflection relations. The maximum resictances increase at the first few cycles through the strain hardening effect. The convergence to the steady loop is rapider, the smaller the axial load or the larger the deflection amplitudes. One of the most remarkable behavior under the cyclic loading is the Bauschinger effect and it is shown clearly by these tests too. The computed results by the Bauschinger model employed here coincide very well with the tested results. At the steady state loop, the Bauschinger or the plastic stresses are reached simultaneously in both tensile and compressive flange.

4.2. Fracture Modes

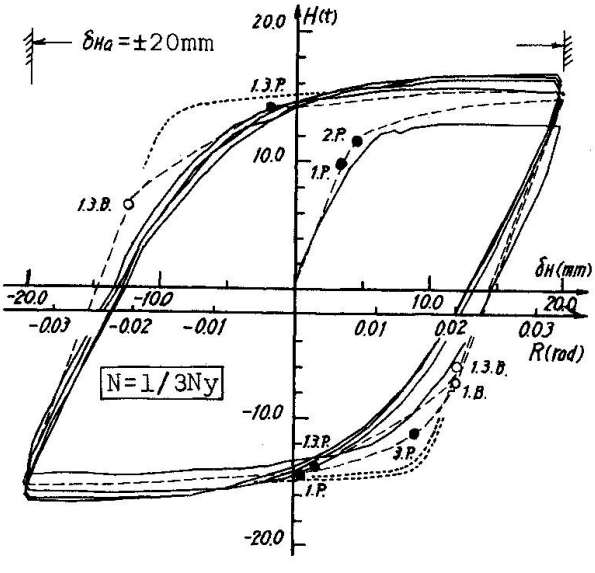

(c) N=1/3Ny, δ_{Ha}=±20mm

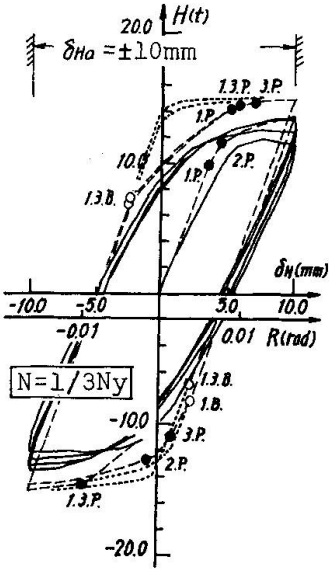

(e) N=1/3Ny, δ_{Ha}=±10mm

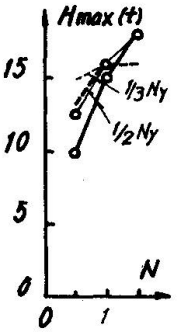

(a) δ_{Ha}=±40mm

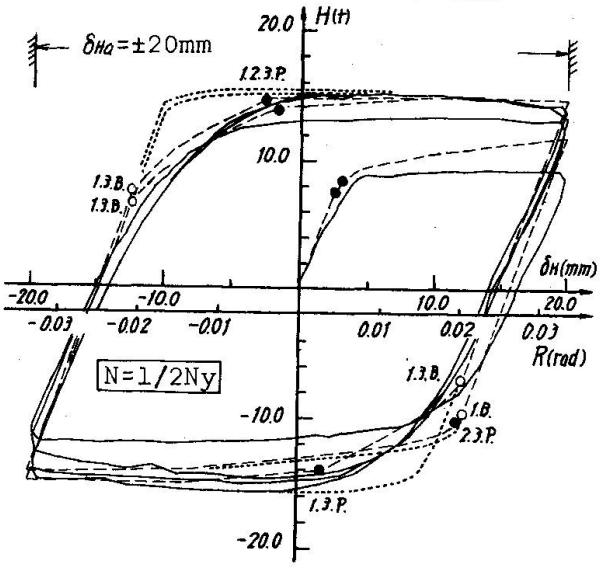

(d) N=1/2Ny, δ_{Ha}=±20mm

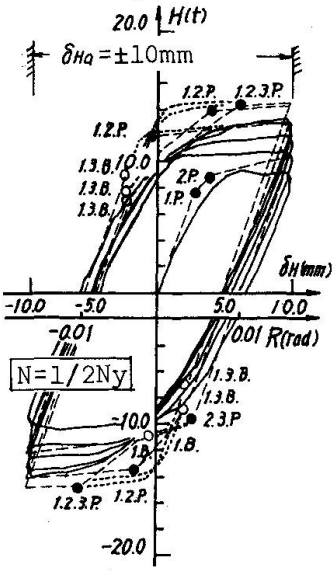

(f) N=1/2Ny, δ_{Ha}=±10mm

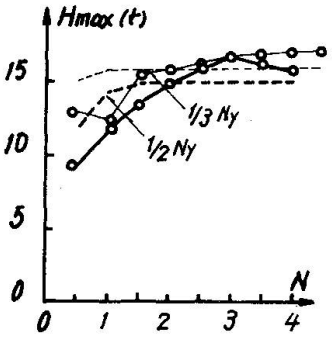

(b) δ_{Ha}=±20mm

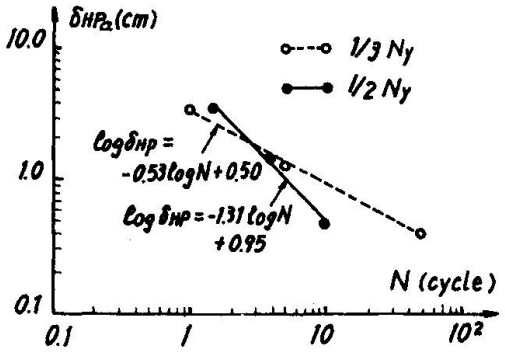

Fig.10

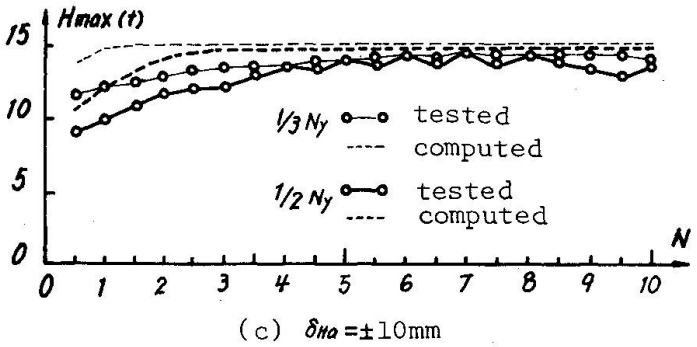

(c) δ_{Ha}=±10mm

Fig.11 Variation of Maximum Resistances

The cyclic loadings are continued until the deterioration of the lateral forces are observed. The local buckling occurs at the column flange in the case of the axial load level of 0Ny or 1/3Ny, whereas it occurs not only at the column flange but also at the column web in the case of 1/2Ny. Two

fracture modes are observed. Under the axial load level of 0Ny or 1/3Ny, the fracture occurred by the tear off of the welded joint, whereas under the axial load level of 1/2Ny, it occurred by the progress of the local buckling. The relationships between the constant plastic deformation amplitudes and the number of cycles until fracture are shown in Fig.10. They lie on the two straight lines in log-log scale corresponding to each fracture mode.

5. BIBLIOGRAPHY

(1) Yamada,M., Shirakawa,K. : Elasto-plastische Biegeformänderungen von Stahlstützen mit I-Querschnitt, Teil II : Wechselseitig wiederholte Biegung unter konstanter Normalkrafteinwirkung, Der Stahlbau, 40. Jahrg., H.3, 1971 S.65-74 u. H.5, 1971 S.143-151.

(2) Zienkiewicz,O.C., Nayak,G.C., Owen,D.R.J. : Composite and overlay models in numerical analysis of elasto-plastic continua, Internl. Symposium Preprint on Foundations of Plasticity, Edited by Sawczuck, Warsaw, 1972, Noordhoff Internl. Publ., Groningen, pp.107-123.

SUMMARY

Constant deflection amplitude tests are carried out on the unit rectangular rigid frames. The remarkable behaviors are the increase of resistances and the Bauschinger effect (Fig. 9). For analysis, the three points model for the cross section (Fig. 4) and the Bauschinger model for the material (Fig. 2) are applied here. The coincidence between tested and computed results are very well. And the both processes are clarified. The relationship between the relative story displacement amplitudes and the number of cycles until fracture are indicated (Fig. 10).

RESUME

Des essais où la grandeur de la déformation est constante sont effectués sur des cadres rectangulaires rigides. Le comportement se caractérise par l'augmentation des résistances et l'effet Bauschinger (Fig. 9). Pour l'analyse, on emploie le modèle à trois points (Fig. 4) pour la section et le modèle Bauschinger (Fig. 2) pour le matériau. Les résultats des essais coïncident très bien avec ceux du calcul. De plus, les deux processus sont expliqués. On indique aussi (Fig. 10) la relation entre la grandeur du déplacement relatif et le nombre de cycles de charge jusqu'à la rupture.

ZUSAMMENFASSUNG

Es werden Versuche mit konstant gehaltener Auslenkung an rechteckigen, steifen Einheitsrahmen gemacht. Bemerkenswert sind die Zunahme des Widerstandes und der Bauschinger-Effekt (Fig. 9). Für die Berechnung werden das Drei-Punkte-Modell für den Querschnitt (Fig. 4) und das Bauschinger-Modell für das Material (Fig. 2) angewendet. Die Uebereinstimmung zwischen den Versuchs- und Rechenresultaten ist sehr gut. Beide Verfahren werden erklärt und die Beziehung zwischen den gegenseitigen Stockwerksverschiebungen und der Anzahl Zyklen bis zum Bruch angegeben (Fig. 10).